Temperature Variation of Magnetic Anisotropy in Pt/Co/AlO_x Trilayers

H. Garad,[1,2] F. Fettar,[1,2,*] F. Gay,[1,2] Y. Joly,[1,2] S. Auffret,[3,4,5] B. Rodmacq,[3,4,5] B. Dieny,[3,4,5] and L. Ortega[6]

[1]*Université Grenoble Alpes, Institut NEEL, F-38000 Grenoble, France*
[2]*CNRS, Institut NEEL, F-38000 Grenoble, France*
[3]*Université Grenoble Alpes, INAC-SPINTEC, F-38000 Grenoble, France*
[4]*CEA, INAC-SPINTEC, F-38000 Grenoble, France*
[5]*CNRS, SPINTEC, F-38000 Grenoble, France*
[6]*Laboratoire de Physique des Solides (CNRS UMR 8502), Batiment 510, Université Paris-Sud, 91405 Orsay, France*

(Received 30 March 2016; revised manuscript received 21 December 2016; published 27 March 2017)

Hysteresis-loop measurements using an extraordinary Hall effect are carried out at different temperatures (4.2–300 K) in Pt/Co/AlO_x trilayers. The AlO_x layer is prepared by plasma oxidation of the Al capping layer during various oxidation times. The samples are subsequently annealed at different temperatures (300 °C–450 °C). Most of the samples exhibit perpendicular anisotropy of increasingly high amplitude as the measurement temperature decreases. In addition, some samples exhibit unusual phenomena such as a temperature-induced reorientation of anisotropy from in plane to out of plane or a large increase of anisotropy at low temperature associated with the onset of exchange bias. The perpendicular magnetic anisotropy, coercivity, thermally induced anisotropy reorientation, and exchange-bias effects are explained by the influence of different chemical bonds, namely, Co—Al, Co—O, and Co—Pt, which appear and/or evolve as a function of oxidation time and annealing temperature. They are linked to the formation of new phases such as CoO or CoPt alloy and to the evolution of the Co/AlO_x, Co/Pt, and Co/CoO interfaces modified by the oxidation time and the interdiffusion between species taking place during the anneals.

DOI: 10.1103/PhysRevApplied.7.034023

I. INTRODUCTION

Spin-orbit interactions are at the origin of magnetic anisotropy [1], which plays an important role in many practical applications of magnetism where the magnetization has to remain oriented along a fixed direction. This is the case in permanent magnets but also in the reference layers of spintronics devices such as spin valves or magnetic tunnel junctions [2]. Because of the importance of anisotropy in areas such as magnetic recording technology and spintronics, many studies have focused on the understanding of anisotropy in layered nanostructures, magnetized either in plane or out of plane, as a function of stack composition, preparation conditions, and measurement temperature. Numerous studies have investigated perpendicular magnetic anisotropy (PMA) in metallic multilayers, particularly those comprising Au/Co or Pt(Pd)/Co bilayers [3–7]. Anisotropy can have bulk and/or interfacial origins: magnetocrystalline, magnetoelastic, interfacial electronic hybridization effect, etc. [8,9]. Roughness at surfaces and interfaces also plays an important role in magnetic anisotropy [10]. The observation of PMA at a magnetic metal-oxide interface [11] such as Co/Al_2O_3 and CoFeB/MgO and its use in out-of-plane magnetized magnetic tunnel junctions for spin-transfer torque–magnetoresistive random-access memory (STT-MRAM) cells [12] attracted considerable attention. From a theoretical point of view, this anisotropy at the Fe(Co)-oxide interface is interpreted in terms of interfacial hybridization effects, particularly those between the $3d_{z^2}$ orbital of the magnetic transition metal and the $2p$ orbitals of oxygen [13,14].

In the Pt/Co(Fe)/MO_x trilayers (M = Al, Ta, Mg, Ru) studied since 2002 [11,15], the interfacial anisotropy is found to be extremely sensitive to the degree of oxidation at the Co(Fe)/MO_x interface. For example, in the plasma-oxidized Pt/Co(0.6 nm)/Al(1.2 nm) trilayers, a maximum of PMA is observed for an intermediate oxidation time $t_{ox} \approx 35$ s of the Al layer and annealing temperature $T_{ann} \approx 300$ C [15]. Underoxidized (shorter oxidation time) or overoxidized (longer oxidation time) interfaces exhibit weaker interfacial PMA (IPMA) at room temperature. It is also found that, upon annealing, oxygen tends to migrate to the Co/AlO_x interface, thereby maximizing the interfacial PMA [15,16]. From an application point of view, this IPMA is very interesting in the context of STT MRAM since it allows obtaining out-of-plane magnetized magnetic tunnel junction with weak Gilbert damping and, therefore, low write current [12]. In these memories, the IPMA exceeds the easy-plane demagnetizing energy thus pulling the storage layer magnetization out of plane. Interestingly, the thermal variation of the IPMA [$K_S(T)$] can be steeper than that of the demagnetizing energy [$-2\pi M_{sat}^2(T)$], so

*farid.fettar@neel.cnrs.fr

that the effective anisotropy $K_{\mathrm{eff}} = [K_S(T)/t] - 2\pi M_{\mathrm{sat}}^2(T)$ may change sign versus temperature (t represents the thickness of the storage layer). This situation yields a reorientation of the anisotropy from out of plane to in plane versus temperature. This thermally induced anisotropy reorientation (TIAR) has already been used to assist the spin-transfer-torque switching in STT MRAM yielding a record value of the figure of merit Δ/I_{c0} [17].

In this paper, low-temperature characterization of the anisotropy in $Pt/Co/AlO_x$ trilayers is performed and discussed in light of the previously investigated structural and chemical properties of these systems [16]. The samples of this study are the same as the ones measured in the previous studies [15,16]. Specifically, we show that, besides the expected trends, the presence of CoO_x and CoPt phases coming from, respectively, the oxidation and annealing process affects (i) the values of coercive (H_C) and anisotropy (H_A) fields at 4.2 K, (ii) the shapes of $H_C(T)$ and $H_A(T)$ curves between 300 and 4.2 K, and (iii) the onset of exchange bias at low temperature together with a large increase in coercivity in some cases of overoxidation of the Al layer. Specifically, the overoxidized sample ($t_{\mathrm{ox}} = 55$ s and $T_{\mathrm{ann}} = 300$ C) exhibits a set of remarkable properties: thermally induced reorientation of anisotropy between RT and 4.2 K, very large coercivity at 4.2 K ($H_C = 1.88$ T) associated with the onset of exchange bias and with the strongest PMA ($H_A = +4.29$ T) at 4.2 K.

II. METHODS AND MATERIALS

In this study, a set of $Si/SiO_2/Pt(3\ \mathrm{nm})/Co(0.6\ \mathrm{nm})/Al(1.6\ \mathrm{nm})$ multilayers are magnetically characterized. They differ by the duration of exposure to the oxygen plasma $t_{\mathrm{ox}} = (15\text{–}25\text{–}40\text{–}55)$ s and by the annealing temperature $T_{\mathrm{ann}} = 20$ C (the as-deposited samples), 300 °C, and 450 °C. More details about deposition and annealing procedures can be found elsewhere [15]. Magnetic characterizations are performed using the extraordinary Hall effect (EHE). In order to determine the coercive field, a first measurement is performed with the magnetic field H_Z (<8 T) applied perpendicular to the sample plane. Before perpendicular measurements, the trilayers are cooled down from 300 to 4.2 K under an out-of-plane field $H_Z = +1$ T in order to induce eventual exchange-bias effects. In the following, the perpendicular normalized EHE_Z (between +1 and −1) is defined by Eq. (1):

$$\mathrm{EHE}_Z(H_Z) = [2\mathrm{EHE}(H_Z) - (\mathrm{EHE}_{\mathrm{max}} + \mathrm{EHE}_{\mathrm{min}})]/\Delta R. \tag{1}$$

Here, $\mathrm{EHE}_{\mathrm{max}}$ and $\mathrm{EHE}_{\mathrm{min}}$ are the maximum and mini mum Hall resistance, respectively, and $\Delta R = \mathrm{EHE}_{\mathrm{max}} - \mathrm{EHE}_{\mathrm{min}}$. Since the EHE is much larger than the normal Hall effect in these samples, the normalized EHE_Z is directly equal to the perpendicular component of the normalized magnetization M_Z. Then a second measurement is performed with field H_X applied parallel to the sample plane with a very small misorientation (1° to 2°) in order to ensure a coherent rotation of the magnetization of the Co moments. The normalized in-plane component of the magnetization M_X is then derived by Eq. (2):

$$M_X(H_X) = [1 - \mathrm{EHE}_Z{}^2]^{0.5}. \tag{2}$$

The anisotropy field H_A, determined from the area between perpendicular and planar EHE measurements, is defined as

$$H_A = 2\int_0^{\infty} dH \cdot [M_Z(H_Z^{\mathrm{mean}}) - M_X(H_X)], \tag{3}$$

where M_Z and M_X are the normalized magnetizations given by Eqs. (1) and (2), respectively, and H_Z^{mean} is the mean magnetic field defined by taking into account the descending and ascending branches of the hysteresis loop.

A $Si/SiO_2/Pt(3\ \mathrm{nm})/Co(0.6\ \mathrm{nm})/Pt(2\ \mathrm{nm})$ reference sample exhibiting perpendicular magnetic anisotropy in the full 4.2–300 K range is also studied for comparison.

III. RESULTS AND DISCUSSION

EHE_Z loops [calculated from Eq. (1)] versus the perpendicular applied magnetic field for different T_{ann} and t_{ox} values, measured at 100 K (right panels) and 4.2 K (left panels), are displayed in Fig. 1. At $T = 100$ K, the largest coercivity is observed for $t_{\mathrm{ox}} = 40$ s for all T_{ann}'s. H_C is the maximum for $T_{\mathrm{ann}} = 300$ C [Fig. 1(f)], similar to what was reported earlier in the same samples at room temperature [15]. Interestingly, for both samples annealed at 300 °C, $t_{\mathrm{ox}} = 15$ s and $t_{\mathrm{ox}} = 55$ s, for which an in-plane anisotropy is observed at $T = 300$ K [15], square hysteresis loops are measured here at the lower temperatures $T = 100$ and 4.2 K [see the right-hand and left-hand panels of Fig. 1, respectively]. For clarity of discussion, the room-temperature EHE data of these two samples are displayed in the insets of Figs. 1(b) and 1(h). For the samples oxidized during the same oxidation times (15 and 55 s), but not annealed, an opening of the hysteresis appears below 100 K. For these two previous as-deposited samples, RT measurements of EHE are also shown in the insets of Figs. 1(b) and 1(h). For instance, the remanence is lower than 3% at 300 K, whereas it reaches (30–100)% at 100 K. These observations indicate that a TIAR takes place in these samples from in plane to out of plane as the temperature is lowered below RT. This TIAR phenomenon is similar to the one reported in Ref. [17] but is here observed below RT.

Concerning the low-temperature data, $T = 4.2$ K, whatever the annealing temperature is, the longer the oxidation time, the larger the H_C. This behavior is also observed in $CoFe/AlO_x/NiFe$ [18] by varying the oxidation time at room temperature. The authors of Ref. [18] claimed that

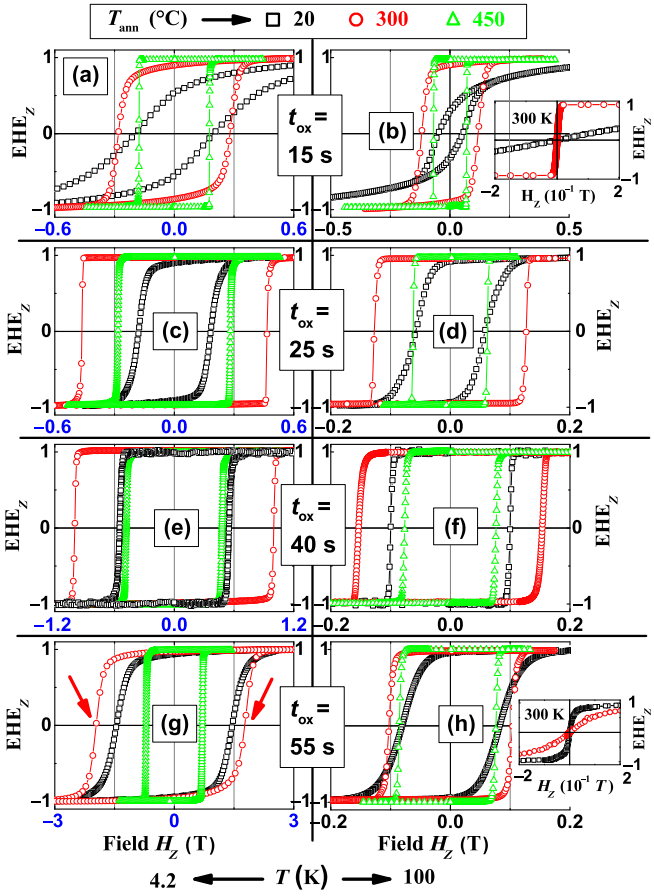

FIG. 1. Normalized extraordinary Hall effects EHE_Z versus the perpendicular applied magnetic field H_Z for $Si/SiO_2/Pt(3\ nm)/Co(0.6\ nm)/Al(1.6\ nm)$ oxidized where (a),(b) $t_{ox} = 15$, (c),(d) 25, (e),(f) 40, and (g),(h) 55 s. The multilayer is as deposited ($T_{ann} = 20$ C) and is annealed at $T_{ann} = 300$ C and 450 °C. The measurement temperature is (left panels) 4.2 K and (right panels) 100 K. See the exchange bias effects at 4.2 K only for the trilayer with $T_{ann} = 300$ C and $t_{ox} = 55$ s [see the arrows in (g)]. RT data are added in (b) and (h) to clarify the discussion (see the text).

localized antiferromagnetic phases of CoO_x and FeO_x are at the origin of this increase in H_C. This explanation may also prevail in our samples. Indeed, as the trilayer is increasingly oxidized in the $t_{ox} = 15$–60 s range, CoO starts forming above $t_{ox} = 40$ s due to oxygen migration along the grain boundaries, as revealed by reflectivity and absorption studies [16].

Exchange coupling between the Co and CoO_x phases can be the main reason for the very large coercivity enhancement observed as the temperature is decreased, particularly for the overoxidized trilayer ($t_{ox} = 55$ s). This interpretation is corroborated by the appearing of exchange bias below 100 K for the sample oxidized during 55 s and annealed at 300 °C. In this sample, H_C (4.2 K) = 1.88 T and H_E (4.2 K) = −0.08 T, as underscored by the arrows in Fig. 1(g). For this sample, magnetic investigations are in progress by modifying the sign, the value, and the configuration (planar versus perpendicular) of the magnetic field before cooling the sample from 400 to 4.2 K, with the aim of getting more details on this exchange-bias phenomenon.

Figure 2 shows the behavior of H_C, as well as the exchange-bias field H_E, as a function of temperature for the different samples. Results for the nonoxidized reference sample is also added for comparison. H_C is larger in all $Pt/Co/AlO_x$ samples than in the reference one, except for the as-deposited sample oxidized during 15 s [Fig. 2(a)]. For the last sample, the low coercivity is explained by the weak perpendicular anisotropy at the Co/AlO_x interface due to the presence of still-numerous oxygen vacancies along the Co/AlO_x interface resulting in poor Co-O electronic hybridization [11,13,15]. This weak IPMA results in an easy-plane anisotropy between 300 and approximately 100 K and weaker coercivity than in Pt/Co/Pt between 100 and 4.2 K. For the other samples, a reinforcement of coercivity is observed compared to Pt/Co/Pt. It is all the more pronounced that t_{ox} is increased. The longer t_{ox}, the larger the curvature in $H_C(T)$ at low temperatures. For fixed t_{ox}, the largest values of $H_C(T)$ are obtained for $T_{ann} = 300$ C. In addition, no exchange bias is observed for all samples except in the overoxidized one ($t_{ox} = 55$ s) and $T_{ann} = 300$ C. The observation of exchange bias in this sample is striking since the nominal thickness of Co is only 0.6 nm.

In-plane $M_X(H_X)$ [calculated from Eq. (2)] magnetization curves, measured at 100 K (right-hand panels) and 4.2 K (left-hand panels) for different T_{ann} and t_{ox} values, are represented in Fig. 3. Clearly, only the as-deposited sample oxidized during 15 s keeps an easy-plane magnetic anisotropy down to 4.2 K. For the other trilayers, a robust PMA is observed. Over the range of annealing temperature investigated, the largest PMA is obtained for $t_{ox} \approx 40$ s at $T = 100$ K and for $t_{ox} \approx 55$ s at $T = 4.2$ K. This result is coherent with the conclusion derived from the data obtained under out-of-plane fields (see Fig. 1). In addition, for both samples for which planar anisotropy at room temperature is observed [15]—namely, $t_{ox} = 55$ s and $T_{ann} = 300$ C, and $t_{ox} = 15$ s and $T_{ann} = 300$ C—an unambiguous PMA is measured at $T = 100$ K and $T = 4.2$ K. A TIAR is observed for these two samples.

To gain deeper insight in the structure of these samples, we perform both x-ray reflectivity (XRR) and x-ray absorption near-edge spectroscopy (XANES) experiments on specific samples. The XRR technique gives information on thickness, roughness, and density for each layer, and the XANES one, carried out at the French CRG BM30B beam line at ESRF (Grenoble, France), is sensitive to the local order around the absorber atoms, here the Co. Figure 4 displays x-ray reflectivity [Fig. 4(a)] and XANES [Fig. 4(b)] data for the two $Pt/Co/AlO_x$ trilayers annealed at 300 °C for $t_{ox} = 15$ and 55 s. From high-quality fittings of XRR data [the blue solid lines in Fig. 4(a)], performed by

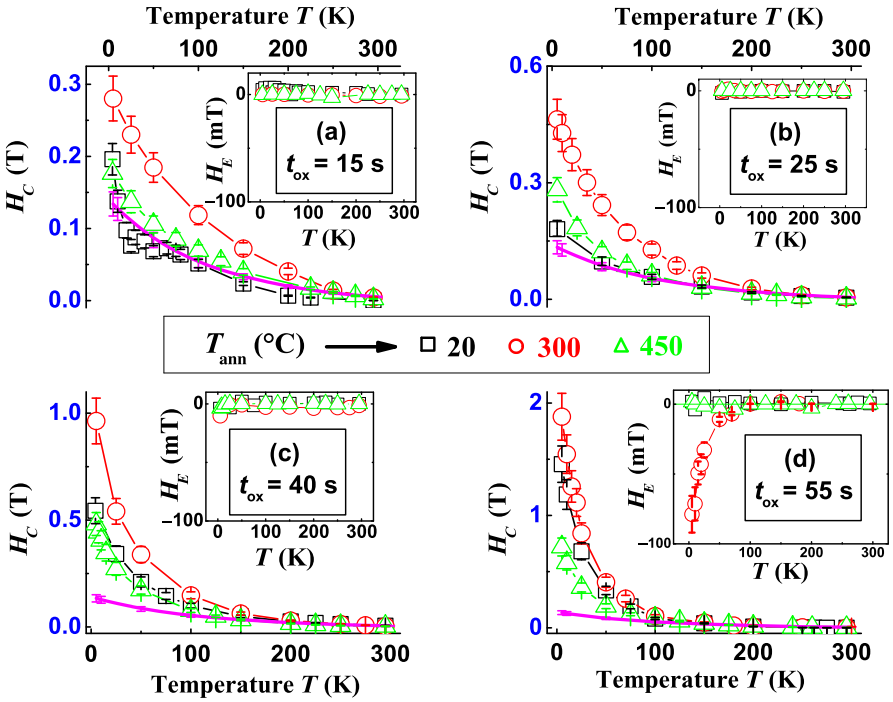

FIG. 2. Coercive field H_C and (insets) the exchange-bias field H_E versus temperature for $Si/SiO_2/Pt(3nm)/Co(0.6nm)/Al(1.6nm)$ oxidized during (a) $t_{ox} = 15$, (b) 25, (c) 40, and (d) 55 s, and annealed at $T_{ann} = (20, 300, 450)$ °C. The data for the $Si/SiO_2/Pt(3\,nm)/Co(0.6\,nm)/Pt(2\,nm)$ reference sample are added for comparison (the full line).

the Bruker LEPTOS software [19], the best corresponding stacks are $Pt/Co/AlO_x$ and $Pt/Co/CoO/AlO_x$ for 15 s, 300 °C and 55 s, 300 °C, respectively. For each layer, the thickness (th), the roughness (rms), and the density (δ) are estimated and merged in Table I. As expected, the oxidation time has a weak influence on the Pt layer, and the deduced parameters (th, rms, and δ) are close to nominal values [$\delta(Pt) = 21.45 \times 10^3$ kg/m^3]. Moreover, the densification and the formation of the alumina layer are observed when t_{ox} is increased from 15 to 55 s. Nevertheless, the lower densities of oxides compared to the bulk values [$\delta(Al_2O_3) = 3.98 \times 10^3$ kg/m^3 and $\delta(CoO) = 6.43 \times 10^3$ kg/m^3] indicate nondense and inhomogeneous layers. Two reasons might be put forward: (i) the oxidation process which seems to be relatively energetic, and (ii) interdiffusion between layers, as seen in the values of rms in Table I, especially for the sample oxidized during $t_{ox} = 55$ s. For this sample, a CoO(0.41 nm) layer is revealed from the x-ray analysis, contrary to the weakly oxidized sample $t_{ox} = 15$ s where no Co—O bonds are detected at the Co-alumina interface.

XANES spectra are very different for CoO-type structure where Co is in a tetrahedral site surrounded by four oxygen atoms and in a Co-metal-type structure, where Co is surrounded by other Co atoms. Because the Co layer is ultrathin (0.6 nm) in our model, corresponding to only two Co planes, the Co bulk experimental spectra are not representative and we have to compare our experiments to simulated spectra, where the unknown is the relative weight between Co in a CoO environment and Co inside a bilayer of Co. We get pretty good agreement [see Fig. 4(b)] explaining the general tendency, despite the fact that the double feature at $E \approx 7725.2$ eV and $E \approx 7728.7$ eV is not seen, which is probably coming from second-neighbor effects not taken into account here (the Co bilayer is supposedly perfect without atoms on both sides). The corresponding fits using the FDMNES code [20] confirm the trends observed from reflectivity measurements. A linear combination of calculated spectra for Co and CoO [see the blue solid lines in Fig. 4(b)] allows us to see that the respective contents of Co and CoO for the $t_{ox} = 55$ s sample are 60% and 40%, whereas a pure Co phase is found for the lowest oxidized sample (15 s). Thus, for the layered structure corresponding to the sample oxidized during 15 s, both the XRR and XANES tools are well suited for describing the topology and chemistry of the trilayer. By contrast, the partially granular structure of the Co entities in the sample oxidized during 55 s, probably makes the XANES determination of the oxide proportion more accurate than the one obtained by reflectivity. The formation of this CoO phase exchange coupled to the Co remaining phase explains the observed exchange bias at low temperature in the $t_{ox} = 55$ s, $T_{ann} = 300$ C sample.

By merging perpendicular and planar measurements, two major results can be emphasized: a spin-reorientation transition as a function of the measurement temperature and the onset of exchange bias at low temperature for the most oxidized sample (55 s). These two phenomena are discussed in more detail below.

(I) Exchange bias is usually reported in samples in which both the ferromagnetic and antiferromagnetic layers are thicker than at least 1 nm. For instance, in NiFe/FeMn bilayers [21], exchange-bias effects appear only for FeMn and NiFe thicknesses larger than 2 and 3 nm, respectively. Different systems

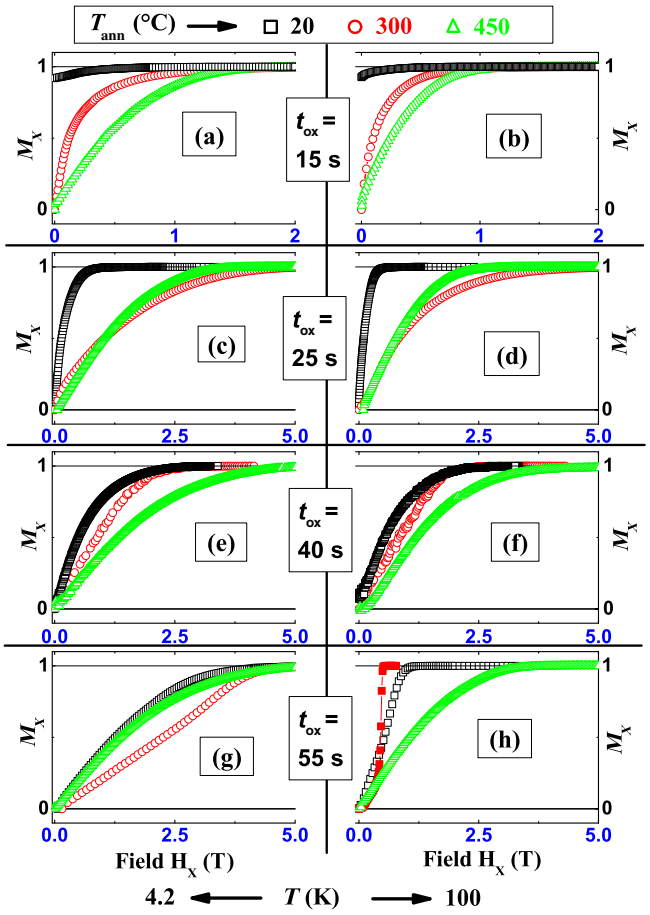

FIG. 3. Variation of the normalized in-plane component of the magnetization M_X versus in-plane applied magnetic field H_X for $Si/SiO_2/Pt(3\ nm)/Co(0.6\ nm)/Al(1.6\ nm)$ oxidized during (a),(b) $t_{ox} = 15$, (c),(d) 25, (e),(f) 40, and (g),(h) 55 s, and annealed at $T_{ann} = (20, 300, 450)$ °C. The measurement temperature is (left panels) 4.2 K and (right panels) 100 K.

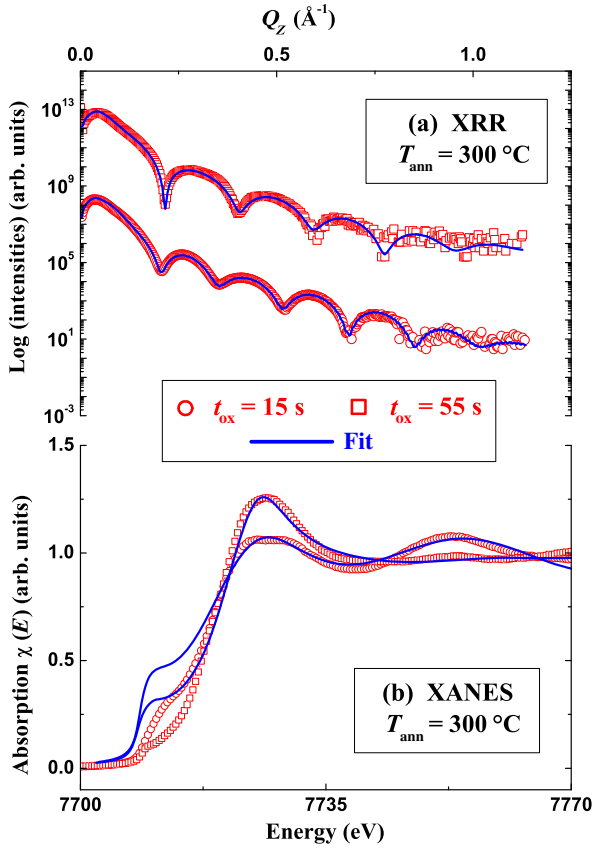

FIG. 4. (a) X-ray reflectivity (XRR) and (b) Co-K edge x-ray absorption near-edge spectroscopy normalized profiles (XANES) data (points) with fittings (blue solid lines) for $Si/SiO_2/Pt(3\ nm)/Co(0.6\ nm)/Al(1.6\ nm)$ oxidized when $t_{ox} = 15$ and 55 s and annealed at $T_{ann} = 300$ C. The curves are shifted vertically in (a) for the sake of clarity, and in-plane polarization geometries are chosen in (b).

can be found in a review paper [22] where antiferromagnetic (AFM) thicknesses in the range of nanometers are used. The onset of exchange bias at 1.4 nm of IrMn is reported at low temperatures ($T < 150$ K) in $IrMn/Co(2.6\ nm)$ [23]. More recently, an exchange bias of 0.1 T is reported at 10 K in $Co(6\ nm)/NiO(1\ nm)$ bilayer [24]. The condition $K_{CoO}t_{CoO} \geq J_{int}$ is required for the onset of exchange bias to insure that the torque exerted by the ferromagnet magnetization on the AFM spin lattice does not drag the AFM spin lattice in its switching, as discussed in a second review paper [25]. For our samples, K_{CoO} is the anisotropy of the CoO layer, t_{CoO} its thickness, and J_{int} the ferromagnetic (Co) or antiferromagnetic (CoO) interface coupling constant. It turns out that CoO has a very large anisotropy at low temperature reaching $K_{CoO} \approx 2.7 \times 10^7$ J/m^3 [26]. Assuming $J_{int} \approx 1$ mJ/m^2 as a reasonable value for the interfacial coupling would yield a critical CoO thickness t_{CoO} of less than a monolayer for the onset of exchange bias at low temperatures. This is typically the order of magnitude for the CoO thickness extracted from structural

TABLE I. Best stacks resulting in XRR adjustments for two samples: $[T_{ann}\ (°C), t_{ox}\ (s)] = [(300, 15), (300, 55)]$. The values th (nm), rms (nm), and δ (10^3 kg/m^3) designate the thickness, roughness, and density for each layer. The th, rms, and δ values are given below for each layer.

T_{ann} (°C)	t_{ox} (s)	Stack
300	15	$Pt[2.97, 0.25, 20.90]/Co[0.59, 0.16, 8.72]/Al_2O_3[1.83, 0.44, 2.03]$
300	55	$Pt[2.96, 0.29, 21.10]/Co[0.08, 0.07, 8.25]/CoO[0.41, 0.15, 4.68]/Al_2O_3[2.47, 0.75, 3.40]$

characterizations. Our observation of exchange bias in the most oxidized sample is therefore a consequence of the very large anisotropy of CoO at low temperatures. From our structural investigations performed with XRR and XANES techniques, in the present overoxidized sample, local CoO patches form during the oxidation process due to oxygen diffusion along grain boundaries. Because of the extremely large anisotropy of CoO ($K_{CoO} \approx 2.7 \times 10^7$ J/m^3) [26], the exchange coupling between the remaining Co layer and the CoO patches can result in dramatically enhanced coercivity and even exchange bias as soon as the size of these patches becomes large enough for their spin lattice not to be entirely dragged during the Co magnetization reversal. In the overoxidized samples annealed at 300 °C, the exchange bias starts appearing below 100 K, whereas the Néel temperature of bulk CoO is 293 K [27]. This result can be explained by the finite-size effect on the Néel temperature of the CoO patches [28] and by the thermally activated dragging of the CoO-patch spin lattice during Co magnetization reversal. Our results can be compared to the ones reported in Ref. [29], where the slope of $H_C(T)$ at decreasing T increases when the CoO thickness is increased in Fe/CoO bilayers. Another explanation for the magnetic properties might be proposed, the disorder effects of layers [30,31]. For instance, in Ref. [31], it was shown that the sputtering deposition pressure for a series of perpendicular anisotropy Co/Pt multilayer films drastically modifies the chemical segregation and grain formation, as well as the surface and interfacial roughness. This characteristic a continuous increase in coercivity with an increasing deposition pressure. For our trilayers, the oxidation time yields a lowering of the roughness (rms) of the Co layer: rms = 1.6 Å and 0.5 Å for the $t_{ox} = 15$ s, $T_{ann} = 300$ C and $t_{ox} = 55$ s, $T_{ann} = 300$ C samples, respectively, as indicated in Table I. As a consequence, the reinforcement of the coercive field when the temperature is lowered cannot be totally explained by the disorder and the roughness, as in the case of Refs. [10,30,31], but mainly due to the CoO phase formation and Co—CoO bonds.

(II) Concerning the anisotropy reorientation transition from in plane to perpendicular from RT down to 4.2 K, both the Co/AlO$_x$ and Co/CoO/AlO$_x$ structures exhibit TIAR, as observed for $t_{ox} = 15$ s, $T_{ann} = 300$ C and $t_{ox} = 55$ s, $T_{ann} = 300$ C trilayers from structural investigations. In fact, TIAR appears for appropriate values of oxidation time, as explained in the Supplemental Material [32]. For further quantitative discussion, the thermal variation of the anisotropy field H_A [see Eq. (3)] is plotted as a function of temperature in Fig. 5 for a different series of samples. The data for the Pt/Co/Pt reference sample are also added for comparison.

For the underoxidized samples ($t_{ox} = 15$ s), a steady increase in PMA is observed with annealing temperature. The as-deposited sample is magnetized in plane over the entire investigated temperature range as previously stated because its easy-plane shape anisotropy overcomes the IPMA at all temperatures. However, upon annealing, the

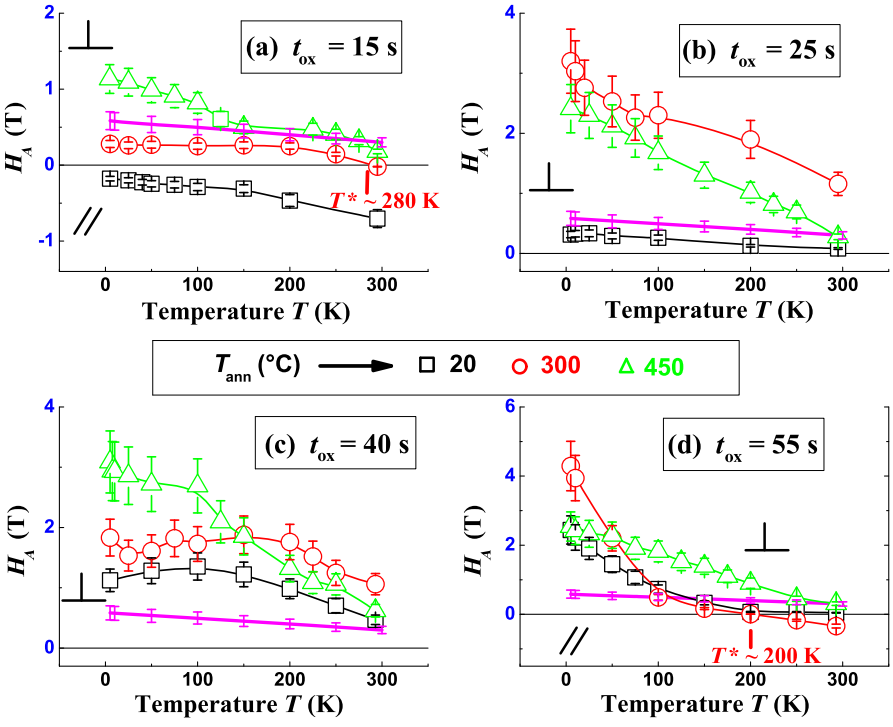

FIG. 5. Temperature dependence of anisotropy field H_A for Si/SiO$_2$/Pt(3 nm)/Co(0.6 nm)/Al(1.6 nm) oxidized for (a) $t_{ox} = 15$, (b) 25, (c) 40, and (d) 55 s, and annealed at $T_{ann} = (20,300,450)$°C. The Si/SiO$_2$/Pt(3 nm)/Co(0.6 nm)/Pt(2 nm) reference is added in a straight line for comparison.

oxygen contained in the bulk of the AlO_x layer tends to migrate towards the Co/AlO_x interface, as revealed by adjustments of the reflectivity and absorption data seen in Fig. 4. As a consequence, the IPMA gradually increases during the annealing process. After annealing at 300 °C, the anisotropy is still weaker than in the reference Pt/Co/Pt reference sample but this is no longer the case in the sample annealed at 450 °C. For the sample annealed at 300 °C, the change of sign of the anisotropy field at about $T^* = 280$ K indicates the TIAR previously mentioned. EHE measurements, for perpendicular as well as planar magnetic fields, for this particular sample ($t_{ox} = 15$ s, $T_{ann} = 300$ C) show the progressive crossover of magnetic anisotropy from in-plane to perpendicular magnetic anisotropy when the temperature is lowered from 300 to 200 K. As revealed by the reflectivity and absorption measurements [16], the CoPt alloy formed by the annealing at 450 °C favors perpendicular magnetic anisotropy which increases when the temperature decreases.

For the sample oxidized for 25 s, the anisotropy field is weak in the as-deposited state [(0.15–0.24) T] and largest after annealing at 300 °C. The decrease of anisotropy field at higher temperature (450 °C) is likely associated with Pt diffusion to the ferromagnetic layer, which reduces the Co—O bonding across the interface responsible for the IPMA [13–15].

In the series oxidized for 40 s, the anisotropy in the as-deposited sample is larger than for the one oxidized 25 s. More oxygen ions have reached the Co/AlO_x interface, as established in Ref. [16], yielding a larger IPMA before any annealing. After annealing, the anisotropy tends to increase. As the temperature decreases, the anisotropy field increases but levels off—or even slightly decreases—at low temperatures. This result can be due to a faster increase of the Co magnetization than of the interfacial anisotropy as the temperature is decreased below 100 K or to some effect related to the bulk anisotropy of CoO, as will be explained further.

In the series of overoxidized samples ($t_{ox} = 55$ s), the sample annealed at 300 °C exhibits a TIAR around $T^* = 200$ K, as previously mentioned. This crossover of magnetic anisotropy from in-plane to perpendicular magnetic anisotropy when the temperature is lowered from 300 to 100 K is detailed for this particular sample in the Supplemental Material [32]. These EHE data illustrate the change of the orientation of the magnetic anisotropy from in-plane (corresponding to $H_A < 0$) to perpendicular (corresponding to $H_A > 0$). The anisotropy field then increases dramatically as the temperature is lowered up to 4.2 T at 4.2 K. This is a surprising result since IPMA is expected to be much reduced in overoxydized samples when oxygen ions start penetrating in the top Co layer forming Co—O—Co planar bonds, as deduced from our XRR and XANES measurements. An explanation for this very large PMA can be found in the bulk anisotropy of CoO, which is extremely large [27]. In CoO, the spins can be rotated much more easily within the (111) planes than out of these planes. Therefore, two anisotropy constants have to be considered in CoO, one related to the spin rotation out of the (111) planes ($K_1 \approx 2.7 \times 10^7$ J/m^3), the other, much weaker, associated with spin rotation within the (111) plane ($K_2 \leq 10^4$ J/m^3) [27]. Upon oxidation of the Pt/Co/Al trilayers, as explained in Ref. [26], the oxygen initially migrates through the Al grain boundaries to the Co/Al interface, then along the Co/Al interface and towards the inner part of the Al grains. Upon further oxidation, the oxygen starts diffusing along the grain boundaries of the Co layer, turning the grain boundaries into CoO. From a structural point of view, this CoO is likely very disordered, but the gradual thickening of the CoO phase at grain boundaries upon oxidation may result in a vertical orientation of the (111) CoO planes which are the dense planes of fcc structure (i.e., perpendicular to the Co/AlO_x interface). As a result of this orientation, the Co magnetization within the grains which is coupled to the CoO spins at the grain boundaries feels a strong net perpendicular anisotropy since pulling the Co magnetization towards the plane of the layer then forces the CoO spins to be locally pulled out of the (111) planes. This scenario can explain the strong increase of anisotropy observed in the overoxidized sample annealed at 300 °C, below the temperature at which exchange bias starts being seen, i.e., below the CoO blocking temperature. For the corresponding sample annealed at 450 °C, the low-temperature strong increase of anisotropy is not observed. This funding can be due to the Pt diffusion through the grain boundaries, which hinders the anisotropy enhancement mechanism described above. Another possible mechanism for this decrease of anisotropy at low temperatures after high-temperature anneal (450 °C) may be a partial deoxidation of the Co layer [16]. This hypothesis leads to a densification of the alumina layer and the formation of a CoPt alloy.

If we now turn back to the case of the sample that is oxidized for 40 s and annealed at 300 °C, a leveling off of the anisotropy increase is observed below approximately 100 K. In this sample, because the oxidation is not as strong as in the samples oxidized for 55 s, the CoO phase may have formed only slightly along the Co/AlO_x interface and not along the grain boundaries. In this case, the (111) orientation of the CoO planes would be parallel to the Co/AlO_x interface and not perpendicular to it. As a result, this CoO phase may favor in-plane anisotropy rather than perpendicular-to-plane anisotropy, resulting in the observed leveling off or even a slight drop of perpendicular anisotropy at low temperature.

IV. SUMMARY AND CONCLUSIONS

In conclusion, by characterizing the low-temperature behavior of the coercive field and anisotropy field in plasma oxidized $Pt/Co/AlO_x$ trilayers annealed at various

annealing temperatures, several interesting phenomena are observed. These particular behaviors are correlated to the physicochemical properties of the systems obtained by quantitative studies of x-ray reflectivity and x-ray absorption near-edge spectroscopy measurements. Specifically, the role of CoO localized phases within the Co-layer grain boundaries and at the Co/AlO_x interface is discussed in relation to the observation of a large increase of the coercivity and anisotropy field at low temperatures associated in one case with the onset of exchange bias. Remarkably, the overoxidized sample ($t_{ox} = 55$ s) annealed at 300 °C exhibits a very large perpendicular anisotropy at 4.2 K [$H_A(4.2\ \mathrm{K}) = 4.29$ T], whereas its magnetization is in plane at RT with a moderate easy-plane anisotropy of $H_A(295\ \mathrm{K}) = -0.34$ T. Upon high-temperature annealing (450 °C), the magnetic properties are influenced by the reduction of the partially oxidized Co layer due to the oxygen ions' migration to the Co/AlO_x interface and by the Pt diffusion inside the Co layer.

ACKNOWLEDGMENTS

This work was partially supported by ERC Advanced Grant MAGICAL No. 669204. We also acknowledge Olivier Proux and Denis Testemale for the technical and scientific supports related to synchrotron experiments.

[1] M. T. Johnson, P. J. H. Bloemen, F. J. A. den Broeder, and J. J. de Vries, Magnetic anisotropy in metallic multilayers, Rep. Prog. Phys. **59**, 1409 (1996).

[2] S. Mao, Tunneling magnetoresistive heads for magnetic data storage, J. Nanosci. Nanotechnol. **7**, 1 (2007); Y. Zheng, Y. Wu, K. Lil, J. Qiu, G. Han, Z. Guo, P. Luo, L. An, Z. Liu, L. Wang, S. G. Tan, B. Zong, and B. Liu, Magnetic random access memory (MRAM), J. Nanosci. Nanotechnol. **7**, 117 (2007).

[3] S. Park, X. Zhang, A. Misra, J. D. Thompson, M. R. Fitzsimmons, S. Lee, and C. M. Falco, Tunable magnetic anisotropy of ultrathin Co layers, Appl. Phys. Lett. **86**, 042504 (2005).

[4] J. Langer, J. Hunter Dunn, A. Hahlin, O. Karis, R. Sellmann, D. Arvanitis, and H. Maletta, Cap layer influence on the spin reorientation transition in Au/Co/Au, Phys. Rev. B **66**, 172401 (2002).

[5] R. Sellmann, H. Fritzsche, H. Maletta, V. Leiner, and R. Siebrecht, Spin-reorientation transition and magnetic phase diagrams of thin epitaxial Au(111)Co films with W and Au overlayers, Phys. Rev. B **64**, 054418 (2001).

[6] J. Kim, J.-W. Lee, J.-R. Jeong, S.-C. Shin, Y. H. Ha, Y. Park, and D. W. Moon, Ultrathin Co films on Pt(111) and the Co-Pt interface investigated by surface magneto-optical Kerr effect and medium-energy ion scattering spectroscopy, Phys. Rev. B **65**, 104428 (2002).

[7] L. Gridneva, A. Persson, M.Á. Niño, J. Camarero, J. J. de Miguel, R. Miranda, C. Hofer, C. Teichert, T. Bobek, A. Locatelli, S. Heun, S. Carlsson, and D. Arvanitis, Experimental investigation of the spin reorientation of Co/Au based magnetic nanodot arrays, Phys. Rev. B **77**, 104425 (2008).

[8] P. Bruno, Tight-binding approach to the orbital magnetic moment and magnetocrystalline anisotropy of transition-metal monolayers, Phys. Rev. B **39**, 865 (1989).

[9] G. H. O. Daalderop, P. J. Kelly, and M. F. H. Schuurmans, Magnetic anisotropy of a free-standing Co monolayer and of multilayers which contain Co monolayers, Phys. Rev. B **50**, 9989 (1994).

[10] S. J. Steinmuller, C. A. F. Vaz, V. Ström, C. Moutafis, D. H. Y. Tse, C. M. Gürtler, M. Kläui, J. A. C. Bland, and Z. Cui, Effect of substrate roughness on the magnetic properties of thin fcc Co films, Phys. Rev. B **76**, 054429 (2007).

[11] S. Monso, B. Rodmacq, S. Auffret, G. Casali, F. Fettar, B. Gilles, B. Dieny, and P. Boyer, Crossover from in-plane to perpendicular anisotropy in $Pt/CoFe/AlO_x$ sandwiches as a function of Al oxidation: A very accurate control of the oxidation of tunnel barriers, Appl. Phys. Lett. **80**, 4157 (2002).

[12] S. Ikeda, K. Miura, H. Yamamoto, K. Mizunuma, H. D. Gan, M. Endo, S. Kanai, J. Hayakawa, F. Matsukura, and H. Ohno, A perpendicular-anisotropy CoFeB-MgO magnetic tunnel junction, Nat. Mater. **9**, 721 (2010).

[13] H. X. Yang, M. Chshiev, B. Dieny, J. H. Lee, A. Manchon, and K. H. Shin, First-principles investigation of the very large perpendicular magnetic anisotropy at Fe|MgO and Co|MgO interfaces, Phys. Rev. B **84**, 054401 (2011).

[14] K. Nakamura, T. Akiyama, T. Ito, M. Weinert, and A. J. Freeman, Role of an interfacial FeO layer in the electric-field-driven switching of magnetocrystalline anisotropy at the Fe/MgO interface, Phys. Rev. B **81**, 220409(R) (2010).

[15] B. Rodmacq, A. Manchon, C. Ducruet, S. Auffret, and B. Dieny, Influence of thermal annealing on the perpendicular magnetic anisotropy of $Pt/Co/AlO_x$ trilayers, Phys. Rev. B **79**, 024423 (2009).

[16] H. Garad, L. Ortega, A. Y. Ramos, Y. Joly, F. Fettar, S. Auffret, B. Rodmacq, B. Diény, O. Proux, and A. I. Erko, Competition between CoO_x and CoPt phases in $Pt/Co/AlO_x$ semi tunnel junctions, J. Appl. Phys. **114**, 053508 (2013).

[17] S. Bandiera, R. C. Sousa, M. Marins de Castro, C. Ducruet, C. Portemont, S. Auffret, L. Vila, I. L. Prejbeanu, B. Rodmacq, and B. Dieny, Spin transfer torque switching assisted by thermally induced anisotropy reorientation in perpendicular magnetic tunnel junctions, Appl. Phys. Lett. **99**, 202507 (2011).

[18] K. S. Yoon, J. Y. Yang, W. J. Choi, C. O. Kim, J. P. Hong, and H. J. Kim, Effect of localized antiferromagnetic phases at interfaces between AlO_x insulating barriers nd $Co_{50}Fe_{50}$ electrodes in magnetic tunnel junctions, Phys. Rev. B **69**, 012407 (2004).

[19] A. Ulyanenkov, Novel methods and universal software for HRXRD, XRR and GISAXS data interpretation, Appl. Surf. Sci. **253**, 106 (2006).

[20] Y. Joly, X-ray absorption near-edge structure calculations beyond the muffin-tin approximation, Phys. Rev. B **63**, 125120 (2001).

[21] R. Jungblut, R. Coehoorn, M. T. Johnson, J. aan de Stegge, and A. Reinders, Orientational dependence of the exchange biasing in molecular-beam-epitaxy-grown $Ni_{80}Fe_{20}/Fe_{50}Mn_{50}$ bilayers, J. Appl. Phys. **75**, 6659 (1994).

[22] J. Nogués and Ivan K. Schuller, Exchange bias, J. Magn. Magn. Mater. **192**, 203 (1999).

[23] M. Ali, C. H. Marrows, M. Al-Jawad, B. J. Hickey, A. Misra, U. Nowak, and K. D. Usadel, Antiferromagnetic layer thickness dependence of the IrMn/Co exchange-bias system, Phys. Rev. B **68**, 214420 (2003).

[24] W. J. Gong, W. Liu, J. N. Feng, D. S. Kim, C. J. Choi, and Z. D. Zhang, Effect of antiferromagnetic layer thickness on exchange bias, training effect, and magnetotransport properties in ferromagnetic/antiferromagnetic antidot arrays, J. Appl. Phys. **115**, 133909 (2014).

[25] W. H. Meiklejohn, Exchange anisotropy—A review, J. Appl. Phys. **33**, 1328 (1962).

[26] J. S. Bae, K. H. Shin, T. D. Lee, and H. M. Lee, Study of the effect of natural oxidation and thermal annealing on microstructures of AlO_x in the magnetic tunnel junction by high-resolution transmission electron microscopy, Appl. Phys. Lett. **80**, 1168 (2002).

[27] A. E. Berkowitz and K.Takano, Exchange anisotropy—A review, J. Magn. Magn. Mater. **200**, 552 (1999).

[28] T. Ambrose and C. L. Chien, Finite-Size Effects and Uncompensated Magnetization in Thin Antiferromagnetic CoO Layers, Phys. Rev. Lett. **76**, 1743 (1996).

[29] R. Abrudan, J. Miguel, M. Bernien, C. Tieg, M. Piantek, J. Kirschner, and W. Kuch, Structural and magnetic properties of epitaxial Fe/CoO bilayers on Ag(001), Phys. Rev. B **77**, 014411 (2008).

[30] C. Fleischmann, F. Almeida, J. Demeter, K. Paredis, A. Teichert, R. Steitz, S. Brems, B. Opperdoes, C. Van Haesendonck, A. Vantomme, and K. Temst, The influence of interface roughness on the magnetic properties of exchange biased CoO/Fe thin films, J. Appl. Phys. **107**, 113907 (2010).

[31] M. S. Pierce, J. E. Davies, J. J. Turner, K. Chesnel, E. E. Fullerton, J. Nam, R. Hailstone, S. D. Kevan, J. B. Kortright, K. Liu, L. B. Sorensen, B. R. York, and O. Hellwig, Influence of structural disorder on magnetic domain formation perpendicular anisotropy thin films, Phys. Rev. B **87**, 184428 (2013).

[32] See Supplemental Material at http://link.aps.org/supplemental/10.1103/PhysRevApplied.7.034023 for (i) diagrams of anisotropy versus oxidation time for $Si/SiO_2/Pt(3\ nm)/Co(0.6\ nm)/Al(1.6\ nm)$ multilayers oxidized during different t_{ox}'s and annealed at $T_{ann} = 300$ C, and (ii) a spin-reorientation-driven temperature in the 150–250 K range for the $Si/SiO_2/Pt(3\ nm)/Co(0.6\ nm)/Al(1.6\ nm)$ multilayer oxidized for $t_{ox} = 55$ s and annealed at $T_{ann} = 300$ C.